



RESEARCH ARTICLE

WILEY

Frequency Domain Electromagnetic mapping for delineating subsurface structures related to the historical port of Emporiae

Albert Casas^{1,2}  | Pere Castanyer³  | Mahjoub Himi¹  | Raul Lovera^{1,2}  |
 Lluís Rivero^{1,2}  | Marta Santos³  | Joaquim Tremoleda³  |
 Alexandre Sendrós¹  | Rubén García-Artigas^{1,2}  | Aritz Urruela¹ 

¹Department of Mineralogy, Petrology and Applied Geology, Earth Sciences Faculty, University of Barcelona, Barcelona, Spain

²Water Research Institute, Universitat de Barcelona, Barcelona, Spain

³Empúries, Museu d'Arqueologia, Girona, Spain

Correspondence

Albert Casas, Department of Mineralogy, Petrology and Applied Geology, Earth Sciences Faculty, University of Barcelona, Martí i Franquès s/n 08028, Barcelona, Spain.
 Email: albert.casas@ub.edu

Funding information

Catalan Agency for Management of University and Research Projects (AGAUR)

Abstract

In recent years, there has been a growing interest in the application of geophysical methods to reconstruct the palaeo-landscapes of sites of special historical interest in support of the planning of archaeological researches. Given the extent of the surface to be investigated, electromagnetic methods have proven to be very suitable for their speed, resolution and versatility for this objective. In particular, coastal areas of the Mediterranean have undergone significant changes in the position of the coastline, because of changes in sea level and sediment inputs that have covered natural harbours used for the establishing colonies.

In this paper, we present the results of a geophysical survey conducted using frequency-domain electromagnetic (FDEM) method carried out to get the geometry of a coastal area near to Emporiae (NE, Spain), which was supposed to form a natural port that was used by Greeks and Romans for its first colonial settlements on the Iberian Peninsula. The results obtained from a dense network of apparent conductivity measurements, supported punctually by other geophysical data (VES and ERT) and boreholes, has allowed us to define the geometry of the basin and confirm the hypotheses of the existence of harbour buried under the coastal and alluvial sediments in the bay close to the remains from Greek and Roman times.

KEYWORDS

ancient port, archaeological exploration, coastal palaeo-landscape, Empúries archaeological site, frequency-domain EMI

1 | INTRODUCTION

Since the beginning of the archaeological investigations in Empúries, the coastal plain existing between the first Greek settlement, named Palaiapolis, and the second one, named Neapolis, has been interpreted that hides in the subsurface a natural port of great significance in the Antiquity (Aquilué et al., 1999). The plain is currently an agricultural land as consequence of the changes in sea level and sedimentation

processes that transformed the coastline. Related to it, there are the remains of a breakwater dated to the 1st century BC (Marcet & Sanmartí, 1989). The study of the port areas of ancient Empúries is probably one of the most illuminating lines of investigation to understand the genesis and evolution of the different settlements established at this site throughout history. For this reason, the current archaeological research project aims to study its port, or rather "its ports," because from the beginning of Empúries' history, there were

This is an open access article under the terms of the Creative Commons Attribution License, which permits use, distribution and reproduction in any medium, provided the original work is properly cited.

© 2021 The Authors. *Archaeological Prospection* published by John Wiley & Sons Ltd.

different port areas, each with its own specific characteristics and adapted to specific needs.

This multidisciplinary project is structured in two main research lines that are completely complementary. The first refers to the archaeological research and involves the excavation in different sectors of Empúries, as well as the study of all the materials recovered in these surveys. The second deals with the geomorphological and palaeoenvironmental reconstruction of these ancient port areas, since knowledge of this is essential to contextualize the data obtained in archaeological interventions. The deep transformation of the landscape around Empúries requires historical interpretation to keep in mind the constant interrelationship between the dynamics of occupation and the dynamics of the landscape.

The study of this historical period focuses most of the interventions and other actions contemplated in this project. The origin and evolution of Emporion is therefore presented as a result of several factors, among which the availability of various port spaces is of particular significance. The case of the so-called “natural harbour” is one of these cases because it was perfectly adapted to the kind of trade developed in the Emporion. Besides, it allowed direct communication with inland territories due to its connection with the estuary of the Fluvià and the northern arm of the Ter.

The archaeological activity during 2018 and 2019 focused on the excavation of the northern quarter of the Greek city, which bordered the natural harbour. This work has recovered the original topography, revealing the cliff boundary that limits with the small harbour bay, above which was the Greek settlement. The original topography had been greatly altered because of the intense sand filling process, which during the late ancient period completely refilled the natural harbour. Communication between the city and the port was made through a ramp located at the northwest corner, where the rock had a softer relief and where there was a small beach. The urban layout of the Greek centre perfectly adapted to the natural topography of the land, which was markedly higher than the port and the coastline.

These archaeological interventions have been complemented with new geophysical surveys in the interior of the natural harbour, as well as various geological surveys, with the aim of gaining a deeper understanding of the characteristics of this port space and establishing the chronology and causes of the subsequent filling process.

Previous researches about sedimentology and evolution of coastline suggested that alluvial sediments of the Fluvià River and sands transported by the sea concealed the historical port of Emporiae (Marquès & Julià, 1983).

The current name of Empúries comes from the Greek term Emporion, which means shopping centre or mall, and faithfully described the purpose of the site, because the city was built initially in the delta of the Fluvià River, crossing several trade routes, and with a natural port, which offered adequate protection to commercial ships. The first Greek settlement is dated to the 6th century BC. The location was in the present town of St. Martin Empúries (Palaipolis) which at that time was surrounded by water, and later was integrated to the coast by an isthmus thanks to the contributions of the sediments of the Fluvià River. In the 5th century BC the

Greeks moved Emporion, from St. Martí Empúries to the south, at an emerged hill in the shoreline (Neapolis). Then, Emporion quickly became one of the most important commercial ports in the Mediterranean (Figure 1).

2 | HISTORICAL FRAMEWORK

The various nuclei of population that, over time, were found in Empúries and its more immediate environment show the importance that this commercial place had during ancient history. During the 7th century BC, the ideal location of the Empordà coast favoured the stable occupation of the various hills in the Empúries area by indigenous communities and the establishing of initial commercial contacts, which soon after, were to culminate in the setting up of the well-known Greek Phocaean Emporion on the promontory of Sant Martí d'Empúries, the Palaia Polis.

The particular morphology and topography of the coastal area, with a small natural bay that served as a port between the island/peninsula of Sant Martí to the north, and the much more wider coastal promontory to the south, allowed that, shortly after the first settlement (Paleapolis), a new Greek city (Neapolis) was built, which kept the name of Emporion.

The origin and evolution of Emporion were always linked to its commercial vocation and its port, as can be seen by the fact that centuries later it also became the Roman gateway to the Iberian Peninsula, initially to solve the war conflict with the Carthaginians and later to contribute to the control and conquest of Hispania. The strategic importance of Empúries at that time is evident from the setting up of a permanent Roman military camp under the shelter of the Greek nucleus, which, once abandoned, was used as a base to create a new Roman city in the early 1st century BC. The settlement was orthogonal in shape and covered a surface area of 22.5 ha, most of which have yet to be discovered. Towards the change of the era, the Greek and the Roman nuclei merged into a single site that we know as municipium Emporiae (Figure 2).

3 | METHODOLOGY

Field geophysical surveys started in 1996 in the framework of a project led by the German Archaeological Institute using a set of different geophysical methods: Vertical electrical soundings (VES), ground probing radar (GPR) and magnetics (Blech et al., 1998). VES showed roughly the structure of the basin and were complemented by a borehole, while GPR and magnetics did not provide results of interest. Subsequently, an ERT survey was carried out but we face logistical difficulties in accessing because it is an agricultural area and the slowness of data acquisition. The location of the previous geophysical measurements is shown in Figure 6. Recently our efforts have been concentrated on frequency-domain electromagnetic method (FDEM) that has shown to be very effective for similar archaeological researches (Bates & Bates, 2000; Tabbagh, 1986).

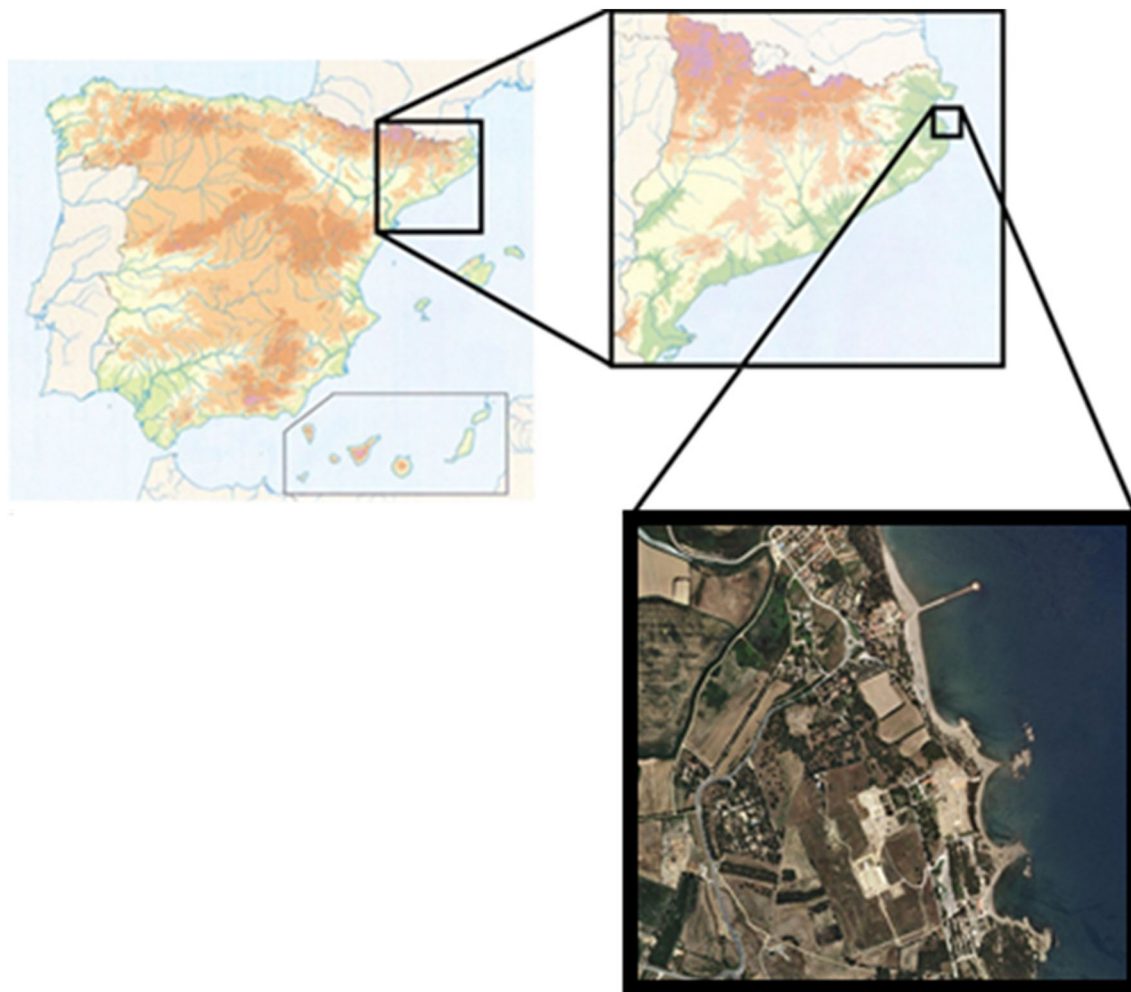


FIGURE 1 General map of Spain and Catalonia showing the location of the archaeological site of Empúries [Colour figure can be viewed at wileyonlinelibrary.com]

According to the objectives of the present study, the geophysical surveys were carried out through gradual stages. First, VES for 1D modelling, ERT for 2D modelling and finally FDEM for mapping.

3.1 | FDEM

The assessment of soil electrical conductivity properties using low frequency induction methods (Keller & Frischknecht, 1966; Wait, 1955) has decades of many successful applications for environmental (Nobes, 1996), hydrogeological (Boaga, 2017) and archaeological studies (Christiansen et al., 2016) among others. In this method, a primary electromagnetic field is induced by the transmitting coil carrying a time-varying electric current at a set frequency, which generates a (primary) magnetic field into the subsurface. The resulting secondary magnetic field is measured together with the primary magnetic field at the receiver coil. The ratio between the secondary and primary magnetic field is recorded as in-phase and quadrature-phase data (Figure 3). The apparent electrical conductivity (ECa) of the bulk soil

can be obtained through the quadrature-phase as a depth weighted electrical conductivity value of a homogeneous medium using the formula given by McNeill (1980):

$$ECa = \frac{4}{f \cdot s^2 \cdot \mu_0} \left(\frac{H_s}{H_p} \right)_{Qu}$$

where f is the frequency (Hz), s is the coil separation, μ_0 is the magnetic permeability of free space ($4\pi \cdot 10^{-7}$ H/m) and $(H_s/H_p)_{Qu}$ is the Qu component of the secondary H_s to primary H_p magnetic field coupling ratio (McNeill, 1980). The formula is an approximation based on the assumption of operating the instrument at low induction number (LIN) and null clearance above the ground conditions. The dimensionless LIN parameter is defined as the ratio between the instrument coil separation and the skin depth δ , where the skin-depth in turn is defined as the distance wherein a plane wave is attenuated by $1/e$ (approx. 37%) of the value at the surface (Spies, 1989).

A Geonics EM31 MK2 ground conductivity meter has been used. The background conductivity noises of the device are 0.1 mS/m for

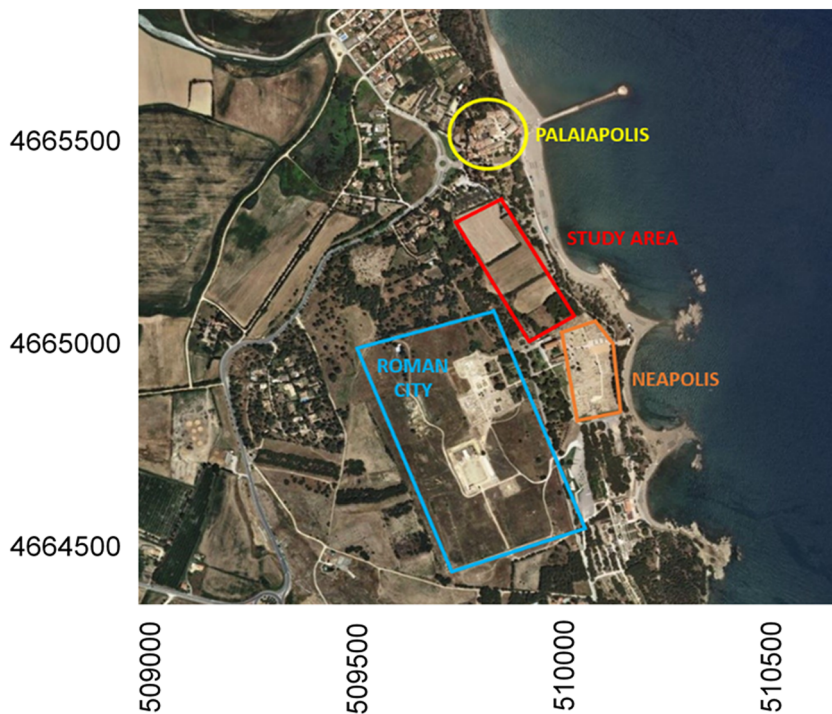


FIGURE 2 Location of the different historical sites referred in the text [Colour figure can be viewed at wileyonlinelibrary.com]

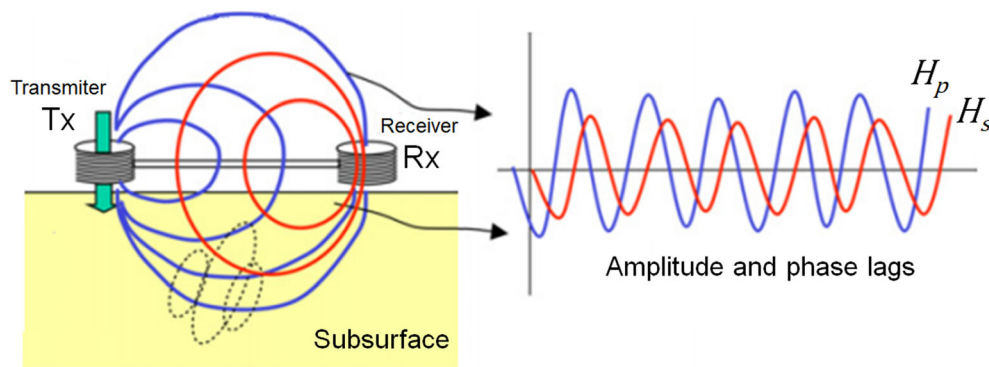


FIGURE 3 Schematic representation of FDEM principles. H_p is the primary field generated the transmitter coil T_x ; H_s is the secondary field recorded at the receiver coil R_x ; dotted lines are Eddy currents (modified from Boaga, 2017) [Colour figure can be viewed at wileyonlinelibrary.com]

the quad-phase signal and 0.03 ppt for the in-phase signal. The instrumental accuracy is 5% for a measurement of the order of 20 mS/m. In the LIN approximation, penetration depth depends of the distance between the coils that is 3.7 m along the horizontal axis and the frequency of the emitted signal that is 9800 Hz. In these conditions, the penetration depths correspond approximately to 3 and 6 m for the horizontal and vertical dipole configurations respectively. The data acquisition is fast if there are not obstacles during the acquisition as was the case in this survey (Figure 4).

A total of 3545 stations were recorded in two dipole configuration modes: horizontal and vertical dipoles. Apparent conductivity measurements were sampled every meter along lines, and the height of the coils was kept at 0.75 m above the ground surface (Figure 5). Data were directly stored to a DL600 data-logger. Repeated measurements were recorded at the beginning and end of each profile to perform corrections for intersection errors (miss ties) that could affect the homogeneity of data during gridding.

3.2 | VES

DC resistivity surveys in the study area were carried out in the framework of project held in 1996 by German Archaeological Institute project (Blech et al., 1998). Five vertical electrical sounding (VES) were recorded along a profile crossing the study area (Figure 6). This preliminary survey was conducted to define thickness of the sediments over the high resistivity basement formed by cretaceous limestones.

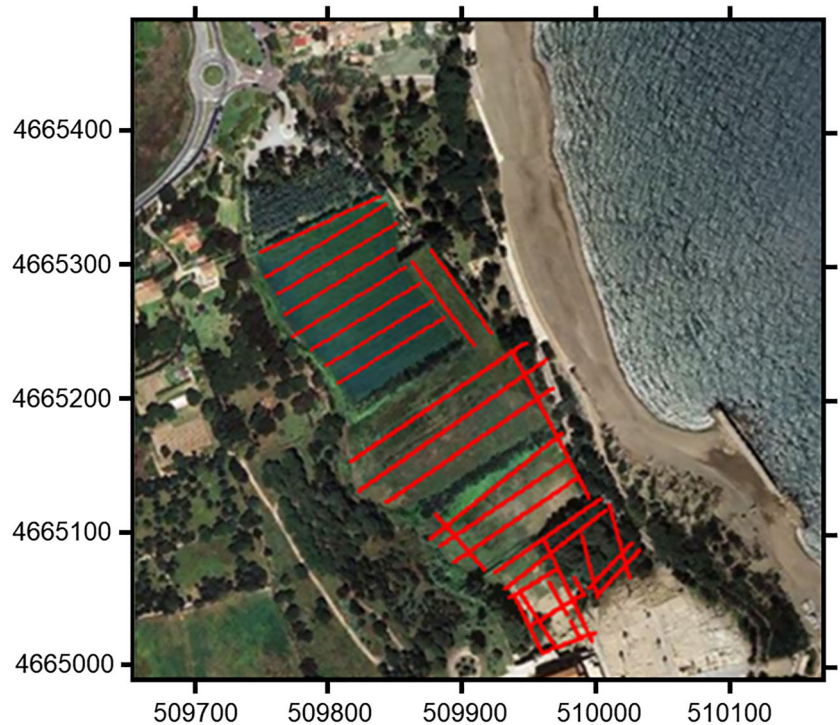
The geophysical equipment used was a DataRes digital resistivity meter from Ambrogeo. A Schlumberger array was selected for this survey because his suitable sensitivity for mapping shallow electrical resistivity variations. The distances between current electrodes (AB) were ranged logarithmically from 1 m to 60 m. This spread was considered long enough to penetrate the sedimentary cover to a depth of about 15 m.

The electrode coupling with the ground was checked before carrying out the measurement for each of the four electrodes at

FIGURE 4 The research area has very favourable conditions for the application of geophysical methods [Colour figure can be viewed at wileyonlinelibrary.com]



FIGURE 5 Location of the FDEM profiles (red lines), distributed along the study area [Colour figure can be viewed at wileyonlinelibrary.com]



each measurement. The IX1D software (Interpex, 2008) was used to process the VES data sets and obtain the subsurface resistivity model. The inversion program incorporates a ridge regression routine to achieve a best fit to the observed data (Inman, 1975). The best fit can be achieved either automatically through the software or manually by adjusting the layer thickness and resistivity values.

To overcome the ambiguity problem in the inversion of resistivity curves, the lithologic information of a borehole was used to build the input models of the inversion process. The borehole S1 was drilled close to VES2 (Figure 6), and some model parameters were fixed during the inversion process according to the available geological data.

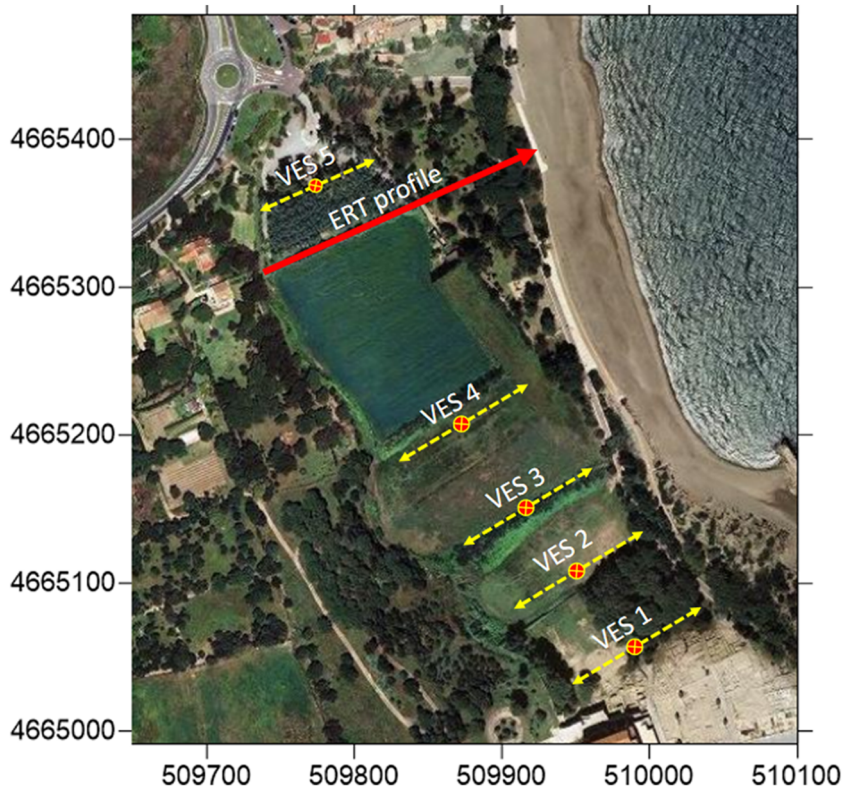


FIGURE 6 Location the centres of the borehole, 5 VES and the 235-m-long ERT profile used to constrain the interpretation of FDEM data [Colour figure can be viewed at wileyonlinelibrary.com]

3.3 | ERT

Five ERT profiles for electrical resistivity imaging were recorded using an IRIS Syscal Pro resistivity meter with 48 electrodes.

All profiles were measured using a Wenner–Schlumberger array and 5-m electrode spacing resulting in a maximum penetration depth of about 20 m. For some profiles, several segments were concatenated to obtain longer profiles as, for instance, the 235-m-long profile showed in the Figure 6. Precise electrode positions were located using a differential GPS.

Apparent resistivity values were first checked for erroneous values that may occur mainly due to bad electrode coupling with the ground that show up as spikes in the apparent resistivity. For all lines, we did then 2D inversion using ram Res2DInv[®] (Geotomo Software, 2010) including the topography. During the inversion process, the root-mean-square value of the difference between experimental data and the updated model response is used as a criterion to assess the convergence (Loke & Barker, 1996). For most lines a root mean square (RMS) data adjustment better than 3% was obtained.

4 | RESULTS

4.1 | FDEM

Apparent electrical conductivity maps have been obtained from FDEM values after statistical data processing and gridding using

Krigging interpolation method and taking into account the anisotropy of sampling (Hansen, 1993). The result was respectively a 5×5 m grid for any coil orientation. Then, colour contour maps have been superimposed over georeferenced aerial images. Apparent conductivity measurements in vertical dipoles showed a wide range of values from 5.5 to 181 mS/m. This effect is interpreted as the result of the high resistivity contrast from 2 to 140 mS/m, between the bedrock (limestones) and the intermediate layer (fine size sand mixed with clay), showing the effect of the subsurface geometry (Figure 7). The higher gradients in the border of the basin can be interpreted as the natural cliffs of limestones that were the geomorphological boundaries of the coastline in the Antiquity. Besides other geophysical limits in both horizontal and vertical dipoles configurations that can be associated with either natural or manmade structures related to the historical port.

4.2 | VES

Experimental apparent resistivity data from all VES curves clearly showed three-layer H type models (Koefoed, 1979) with a thin high resistivity top layer, interpreted as a soil cover, an intermediate layer of fine size sand mixed with clay of low electrical resistivity and thicknesses ranging from 5 to 10 m and a high resistivity layer at the bottom interpreted as the Cretaceous limestone. The inverted model of VES 2, constrained by the geological log from the borehole S 1, drilled few meters apart, is shown in Figure 8.

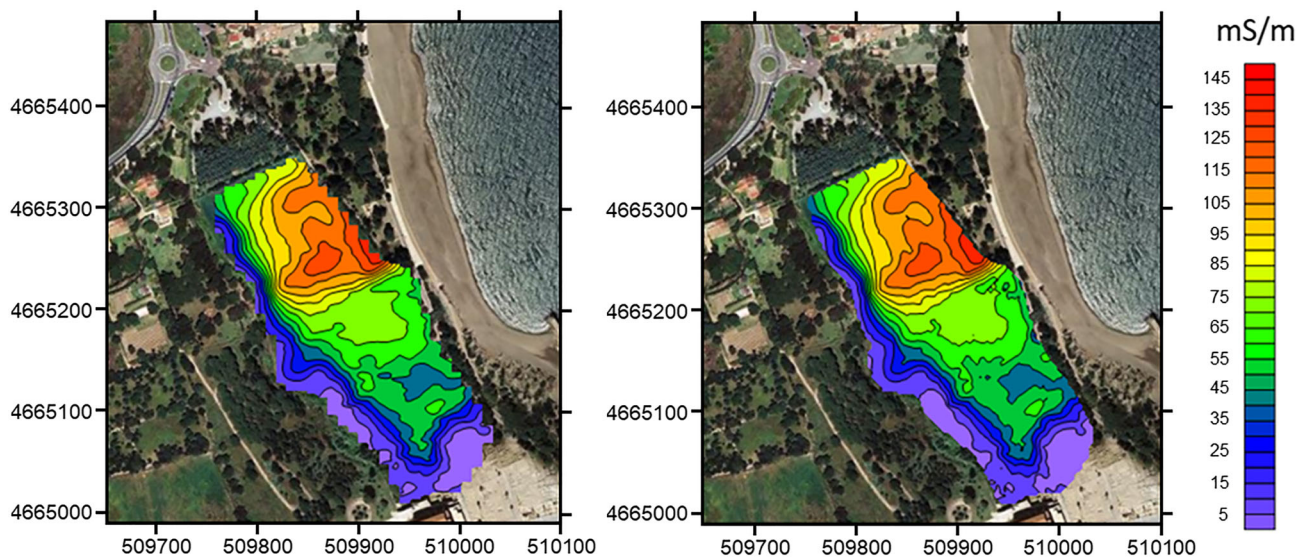


FIGURE 7 Apparent conductivity maps for horizontal dipoles (left) and vertical dipoles (right) from the interpolation of FDEM. Units are expressed in mS/m [Colour figure can be viewed at wileyonlinelibrary.com]

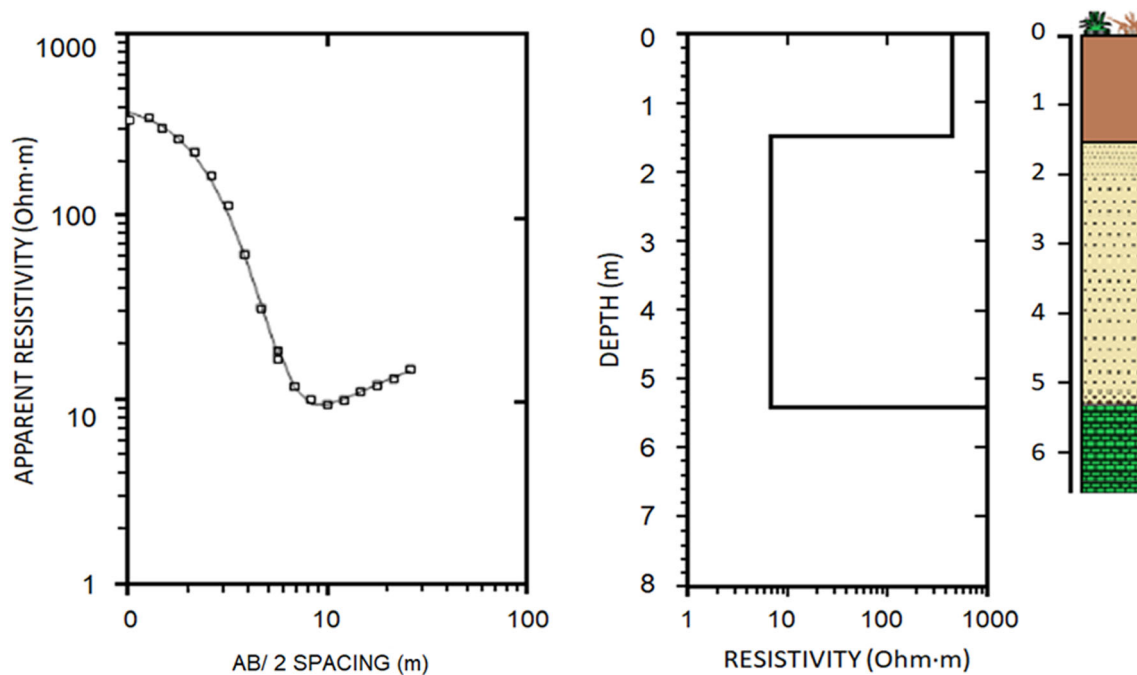


FIGURE 8 Inversion of the three-layer VES 2 and geological log of the borehole S 1 drilled next to VES centre. Top layer: brown soil, intermediate layer: fine size sand mixed with clay; bottom layer: limestone [Colour figure can be viewed at wileyonlinelibrary.com]

4.3 | ERT

Two-dimensional electrical resistivity cross sections showed the same subsurface structure of three different layers with $\rho_1 > \rho_2 < \rho_3$. The upper layer has an almost constant thickness (1.5 m) and resistivity (250 $\Omega \cdot m$) but the thickness of intermediate layer of low resistivity changes laterally over a high resistivity basement (Figure 9).

5 | INTERPRETATION AND DISCUSSION

Usually the interpretation of FDEM data for archaeological surveys is based only on mapping and delineation of the borders of anomalies. Nevertheless, in this study, we have tried to get as much information as possible by a constrained inversion of FDEM data (Benech et al., 2016). The characteristics of sedimentary filling and depth of the limestone substrate have been interpreted from the solution

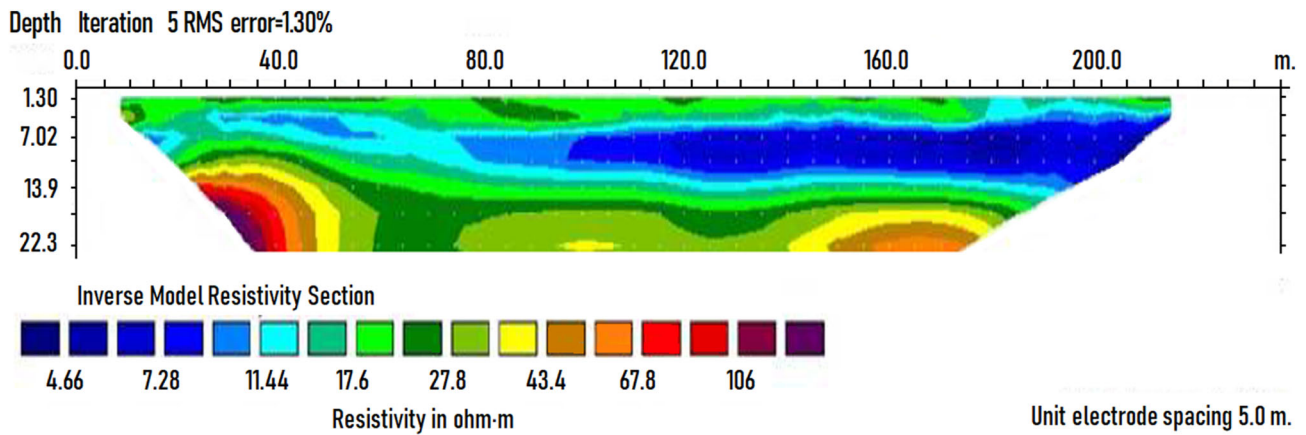


FIGURE 9 Cross-section of the ERT profile which location is showed on Figure 6 [Colour figure can be viewed at wileyonlinelibrary.com]

of the 1D direct and inversion problem of synthetic models based on the geological log of the boreholes and the models (depths and electrical resistivities) obtained from the inversion of the five vertical electrical soundings (VES) distributed along the basin.

The map of electrical conductivity anomalies for the configuration of vertical dipoles (Figure 7) can be interpreted as the result of the variation of the depth of the bedrock substrate, so the areas of greater depth would correspond to those with the highest values of electrical conductivity. As in the position of the S1 borehole with electrical conductivity values of 55 mS/m the depth to the bedrock was 5.2 m, it could be assumed that in the areas of greater electrical conductivity, the depth of the bedrock should be greater.

EMI measurements return an apparent electrical conductivity that represents an integrated average of the electrical conductivity distribution over a certain soil volume. The reconstruction of this distribution is often difficult due to the intrinsic non-uniqueness of interpretation of a layered subsurface. In order to get a greater approximation of the depth model, we decided to carry out an inversion of the experimental data, despite the limitations imposed by the limit of the investigation depth and the maintenance of the operating conditions at low induction number. Most EMI inversion algorithms use a 1D forward model based on either the linear cumulative sensitivity (CS) functions proposed by McNeill (1980) or non-linear full solution (FS) forward models based on Maxwell's equations. Any inversion process aims to find a plausible model of the subsurface, which adequately fits the observed data within the limits of the data uncertainty. The process consists of two components: forward modelling and inversion. Forward modelling generates the response of a specific synthetic model, whereas inversion automatically changes the model to reduce the misfit between measured and forward-modelled data.

The initial model was a three-layer model with the following electrical conductivity values derived from the constrained inversion of VES 2.

4 mS/m for the first layer (soil)

140 mS/m for the second layer (fine size sand mixed with clay)

3 mS/m for the third layer (limestone)

The thickness of the first layer kept fix to 1.5 m, and the thickness of the second layer was considered the free variable.

Taking into account that some authors (Callegary et al., 2007; Christiansen et al., 2016; Deidda et al., 2014; Reid & Howlett, 2001, among others) question the accuracy of the linear cumulative sensitivity (CS) with respect to the non-linear full solution (FS) we have carried out a comparison of the results by both two methods for the three-layer model corresponding to the S1 well that coincides with the VES2. For the calculation of the direct response of the model from the non-linear full solution (FS) the software FDEMTOOLS (Deidda et al., 2020) has been used. The results obtained have been quite similar, 54 mS/m for the CS method and 56.7 mS/m for the FS method, and very approximate to the experimental measurement of apparent electrical conductivity of 55 mS/m.

Therefore, due to their simplicity and efficiency, compared with non-linear full solution of forward models based on Maxwell's equations, the linear cumulative sensitivity functions have been used. The response of the model was calculated following the formula given by McNeill (1980):

$$\sigma_a = \sigma_1 [1 - R_V(z_1)] + \sigma_2 [R_V(z_1) - R_V(z_2)] + \sigma_3 [R_V(z_2)]$$

where σ_a is the bulk apparent conductivity of the layered earth, σ_1 , σ_2 and σ_3 are the electrical conductivities of the top, intermediate and bottom later, z_1 and z_2 the depths to the second layer and third layer, respectively. R_V or R_H are the relative contributions of vertical and horizontal components to the secondary magnetic field or apparent conductivity from all material below a depth z given by

$$R_V(z) = \int_z^\infty \vartheta_V(z) dz \quad \text{and} \quad R_H(z) = \int_z^\infty \vartheta_H(z) dz$$

where

$$\vartheta_V(z) = \frac{4z}{(4z^2 + 1)^{3/2}} \quad \text{and} \quad \vartheta_H(z) = 2 - \frac{4z}{(4z^2 + 1)^{3/2}}$$

The functions $\vartheta(z)$ and $R(z)$ define the relative influence of current flow as a function of depth a z is the depth divided by the intercoil space. Always following McNeill (1980), the functions $R_V(z)$ and $R_H(z)$ can be easily calculated by

$$R_V(z) = \frac{1}{(4z^2 + 1)4^{1/2}} \quad \text{and} \quad R_H(z) = \int_z^\infty \vartheta_H(z) dz$$

Then, FDEM apparent electrical conductivity data close to borehole S1 have been inverted keeping invariant all the parameters of the model except the thickness of the second layer (Guérin et al., 1996). The apparent electrical conductivity of the model for vertical dipoles was 55.80 mS/m whereas the observed apparent conductivity was 56.2 mS/m.

The same 1D inversion process has been applied to all FDEM conductivity values and an iso-depth map of the basement has been generated (Figure 10). The iso-depth map shows the existence of structures that can be assumed as platforms and channels. This interpretation is following the hypothesis advanced by the archaeologists that is reproduced (Figure 11) and with a borehole drilled that found the limestone substrate at 5.20 m depth. Besides, the radiocarbon dating of plant remains at 4.80 m depth gave an age of 2020 \pm 70 years, which is consistent with the historical period of the port.

After the depth to basement model was built from the inversion of FDEM data, two new boreholes were drilled further to the centre of the basin. In each of the boreholes the basement was reached, at a depth of 8.30 m and 9.30 m in S2 and S3 boreholes, respectively. These results are in good agreement with the depths deduced by the model at both points. The correlation between the depths obtained in the surveys and those deduced from the inversion of the apparent electrical conductivity values is shown in the graph attached to Figure 10 with a $R^2 = 0.98$.

As regards the archaeological diggings carried out in the framework of the research project the most important action focuses on the northern quarter of the Greek city. The aim was recovering the ancient topography and understanding the connection of the city with

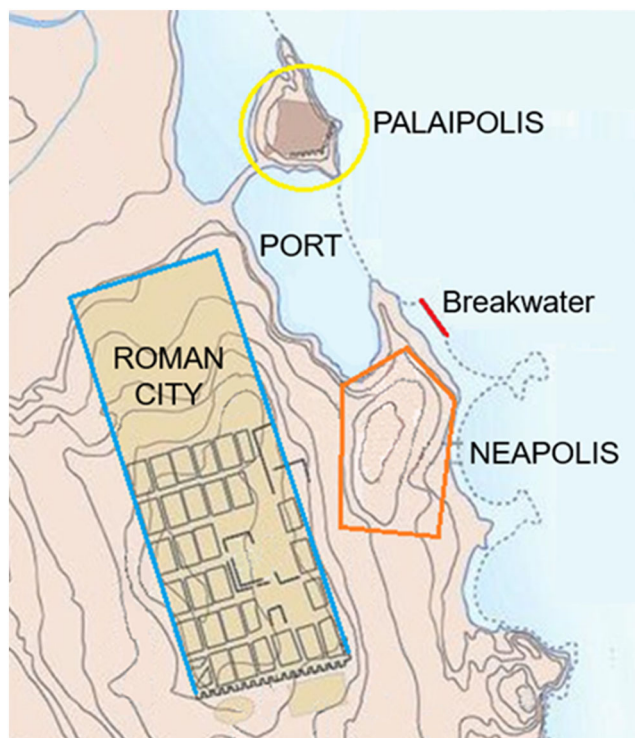


FIGURE 11 Reconstruction of the landscape based on the previous archaeological hypothesis and the geophysical results presented in this paper [Colour figure can be viewed at wileyonlinelibrary.com]

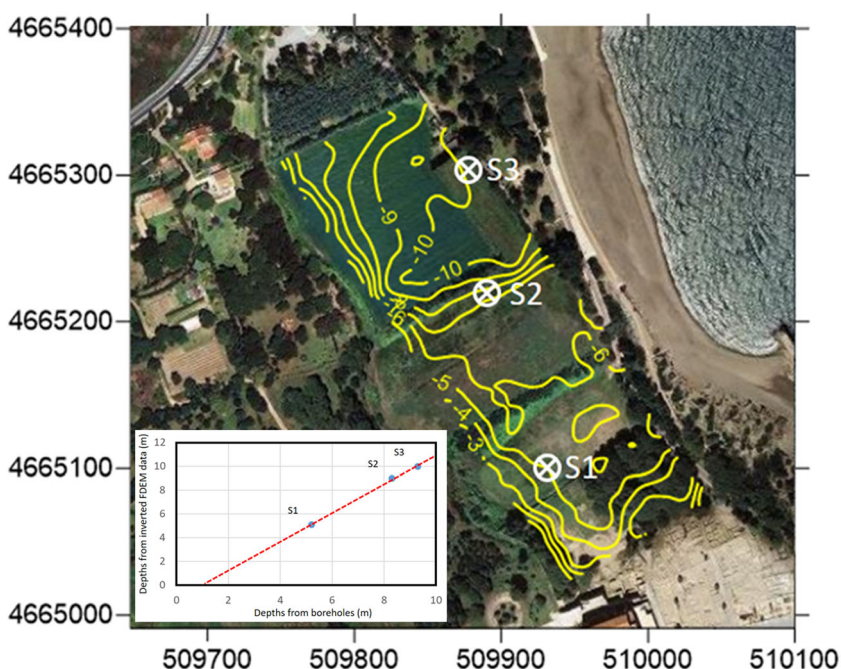


FIGURE 10 Map of depth to bedrock generated by kriging from the inverted EMI apparent electrical conductivity (Eca) in vertical dipole orientation. The diagram included inside the frame shows the comparison between the observed vs. predicted depth to bedrock for the three boreholes [Colour figure can be viewed at wileyonlinelibrary.com]



FIGURE 12 Picture showing a series of ridges artificially excavated in the rock that have been exposed during the recent archaeological at the meridional limit of the basin that can be interpreted as the remains of the docks of the Greek Port [Colour figure can be viewed at wileyonlinelibrary.com]

the old natural port. Recent archaeological excavations carried out at the meridional boundary of the basin have exposed a series of artificially excavated rocky ridges, which can be interpreted as the remains of the docks of the Ancient Greek Port (Figure 12).

Besides, archaeological intervention in the northern quarter of the Neapolis has been completed with the excavation of the northeastern landfill of the Greek city, on the coastal facade itself. This area, which is currently outside the archaeological complex, in ancient times, was part of the same urban centre. At some points, the stratigraphic sequence made it possible to identify different successive levels of occupation, as well as some sediments that directly covered the natural rock. The ceramic materials associated with these strata confirm that the occupation of this sector occurred during the initial stage of the Neapolis, starting in the second half of the 6th century BC (Marcet & Sanmartí, 1989).

6 | CONCLUSIONS

The results obtained in this study indicate that shallow electromagnetic induction is a cost-effective alternative for mapping the buried palaeo-landscape related to harbours and coastal plains laying over a high resistivity basement. In our case, the existence of a thin low electrical conductivity layer overlaying a fine sand mixed with clay, the resolution of subsurface parameters is much better than in the opposite case of a highly conductive layer overlaying a moderately conductive layer.

Particularly, the geophysical images and resulting interpretation from data obtained in this study confirmed the existence of a

well-defined basin between the Greek archaeological sites named Palaiapolis and Neapolis.

Then, we can conclude that the basin was used in Antiquity as a natural port as has been suggested by the Archaeologist from long ago without conclusive evidence. Nevertheless, further archaeological diggings and geophysical surveys should be conducted.

ACKNOWLEDGEMENTS

The assistance provided by Professor Gian Piero Deidda (Università degli Studi di Cagliari, Italy) is greatly appreciated.

This research was funded by project (CLT009/18/0089) The Port Areas of the Old Empúries of the Catalan Agency for Management of University and Research Projects (AGAUR).

CONFLICT OF INTEREST

The authors declare that there is no conflict of interest.

DATA AVAILABILITY STATEMENT

The data that support the findings of this study are available on request from the corresponding author

ORCID

Albert Casas <https://orcid.org/0000-0002-4964-1226>

Pere Castanyer <https://orcid.org/0000-0001-5080-3571>

Mahjoub Himi <https://orcid.org/0000-0003-1419-6676>

Raul Lovera <https://orcid.org/0000-0001-8338-7826>

Lluís Rivero <https://orcid.org/0000-0003-0475-2333>

Marta Santos <https://orcid.org/0000-0002-1542-9040>

Joaquim Tremoleda <https://orcid.org/0000-0002-2699-7318>

Alexandre Sendrós  <https://orcid.org/0000-0002-0716-9322>

Rubén García-Artigas  <https://orcid.org/0000-0002-9347-1615>

Aritz Urruela  <https://orcid.org/0000-0003-3349-8266>

REFERENCES

- Aquilué, X., Castanyer, P., Santos, M., & Tremoleda, J. (1999). *Empúries*. Tarragona: Guies del Museu d'Arqueologia de Catalunya.
- Bates, M. R., & Bates, C. R. (2000). Multidisciplinary approaches to the geoarchaeological evaluation of deeply stratified sedimentary sequences: Examples from Pleistocene and Holocene deposits in Southern England, UK. *Journal of Archaeological Science*, 27, 845–858. <https://doi.org/10.1006/jasc.2000.0584>
- Benech, C., Dabas, M., Simon, F. X., Tabbagh, A., & Thiesson, J. (2016). Interpretation of shallow electromagnetic instruments resistivity and magnetic susceptibility measurements using rapid 1D/3D inversion. *Geophysics*, 81, E103–E112. <https://doi.org/10.1190/geo2014-0549.1>
- Blech, M., Marzoli, D., Burjachs, F., Buxó, R., Casas, A., Giralt, S., & Rambaud, F. (1998). Interdisziplinäre prospektionen im Ampurdán: vorbericht der kampagne september 1996. *Madriider Mitteilungen*, 39, 99–120.
- Boaga, J. (2017). The use of FDEM in hydrogeophysics: A review. *Journal of Applied Geophysics*, 139, 36–46. <https://doi.org/10.1016/j.jappgeo.2017.02.011>
- Callegary, J. B., Ferré, T. P. A., & Groom, R. W. (2007). Vertical spatial sensitivity and exploration depth of low-induction-number electromagnetic-induction instruments. *Vadose Zone Journal*, 6, 158–167. <https://doi.org/10.2136/vzj2006.0120>
- Christiansen, A. V., Pedersen, J. B., Auken, E., Sørensen, N. E., Holst, M. K., & Kristiansen, S. M. (2016). Improved geoarchaeological mapping with electromagnetic induction instruments from dedicated processing and inversion. *Remote Sensing*, 8, 1022. <https://doi.org/10.3390/rs8121022>
- Deidda, G. P., Díaz de Alba, P., Fenu, C., Lovicu, G., & Rodríguez, G. (2020). FDEMTTOOLS: A MATLAB package for FDEM data inversion. *Numerical Algorithms*, 84, 1313–1327. <https://doi.org/10.1007/s11075-019-00843-2>
- Deidda, G. P., Fenu, C., & Rodríguez, G. (2014). Regularized solution of a nonlinear problem in electromagnetic sounding. *Inverse Problems*, 30, 125014. <https://doi.org/10.1088/0266-5611/30/12/125014>
- Geotomo Software. (2010). RES2DINV ver. 3.59. Rapid 2-D Resistivity & IP inversion using the least-squares method for Windows XP/Vista/7, Malaysia, pp. 1–157.
- Guérin, R., Méhény, G., Rakotondraso, D., & Tabbagh, A. (1996). Interpretation of slingram conductivity in near-surface geophysics using a single parameter fitting with 1D model. *Geophysical Prospecting*, 44, 233–249. <https://doi.org/10.1111/j.1365-2478.1996.tb00148.x>
- Hansen, R. O. (1993). Interpretative gridding by anisotropic kriging. *Geophysics*, 58, 1400–1551.
- Inman, J. R. (1975). Resistivity inversion with ridge regression. *Geophysics*, 40, 798–817. <https://doi.org/10.1190/1.1440569>
- Interpex. (2008). *IX1D v2 instruction manual* (pp. 1–67). USA: Interpex Limited.
- Keller, G. V., & Frischknecht, F. C. (1966). *Electrical methods in geophysical prospecting*. New York: Pergamon Press.
- Koefoed, O. (1979). *Geosounding principles, 1. Resistivity sounding measurements*. Amsterdam: Elsevier Science Publishing Company.
- Loke, M. H., & Barker, R. D. (1996). Rapid least-squares inversion of apparent resistivity pseudosections using quasi-Newton method. *Geophysical Prospecting*, 48, 181–152.
- Marcet, R., & Sanmartí, E. (1989). *Empúries*. Diputació de Barcelona.
- Marquès, M. A., & Julià, R. (1983). Coastal problems in Alt Emporadà Area (NE Catalonia, Spain). In E. C. F. Bird & P. Fabbri (Eds.), *Coastal problems in Mediterranean Sea* (pp. 83–93). International Geographical Union (IGU), Bologna, Commission on the Coastal Environment.
- McNeill, J. D. (1980). *Electromagnetic terrain conductivity measurement at low induction numbers. Technical Note TN-6* (pp. 1–15). Mississauga, ON, Canada: Geonics Ltd.
- Nobes, D. C. (1996). Troubled waters: Environmental applications of electrical and electromagnetic methods. *Surveys in Geophysics*, 17, 393–454. <https://doi.org/10.1007/BF01901640>
- Reid, J. E., & Howlett, A. (2001). Application of the EM-31 terrain conductivity meter in highly-conductive regimes. *Exploration Geophysics*, 32, 219–224. <https://doi.org/10.1071/EG01219>
- Spies, B. R. (1989). Effective depth of exploration in electro-magnetic sounding methods. *Geophysics*, 54, 872–888. <https://doi.org/10.1190/1.1442716>
- Tabbagh, A. (1986). Applications and advantages of the Slingram electromagnetic method for archaeological prospecting. *Geophysics*, 51, 576–584. <https://doi.org/10.1190/1.1442112>
- Wait, J. R. (1955). Mutual electromagnetic coupling of loops over a homogeneous ground. *Geophysics*, 20, 630–637. <https://doi.org/10.1190/1.1438167>

How to cite this article: Casas, A., Castanyer, P., Himi, M., Lovera, R., Rivero, L., Santos, M., Tremoleda, J., Sendrós, A., García-Artigas, R., & Urruela, A. (2021). Frequency Domain Electromagnetic mapping for delineating subsurface structures related to the historical port of Emporiae. *Archaeological Prospection*, 1–11. <https://doi.org/10.1002/arp.1834>